

MRL 817-104 (TR)c.2.

MRL 817-104 (TR)c.2



Energy, Mines and  
Resources Canada

Énergie, Mines et  
Ressources Canada

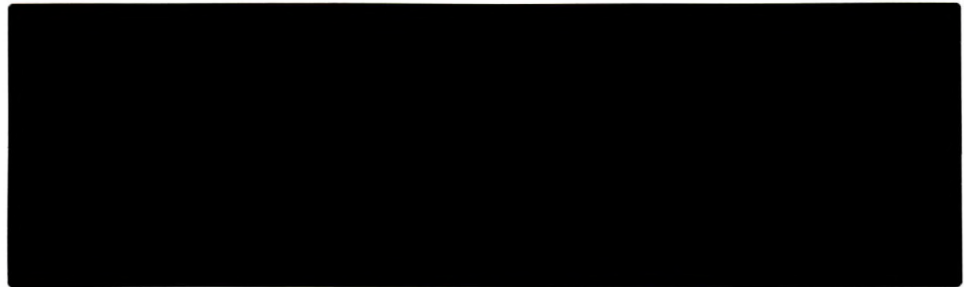
# CANMET

Canada Centre for  
Mineral and Energy  
Technology

Centre canadien de la  
technologie des  
minéraux et de l'énergie

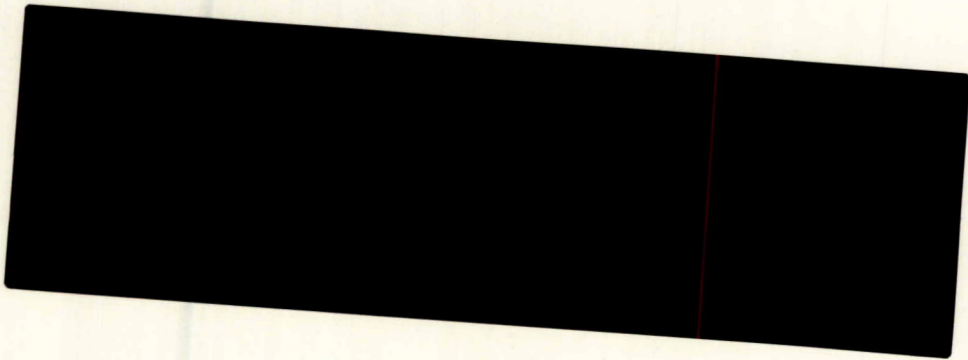
**Mining  
Research  
Laboratories**

**Laboratoires  
de recherche  
minière**



Canada 





Canmet Information  
Centre  
D'information de Canmet

JAN 31 1997

555, rue Booth ST.  
Ottawa, Ontario K1A 0G1

1-7987709 c.2  
CPUB

**ANISOTROPIC PROPERTIES STUDY OF LAC DU BONNET**

**GRANITE SPECIMENS: REPORT #4** 1-7987709

*R. Jackson*

MRL 87-104(TR) c.2  
CPUB

c.2  
CPUB →

1-798 7709 e.2  
CPUB

ANISOTROPIC PROPERTIES STUDY OF LAC DU BONNET GRANITE SPECIMENS:  
REPORT #4

by  
Rand Jackson\*

ABSTRACT

Compressive and shear wave velocity measurements, as well as uniaxial compression testing, was conducted on samples obtained from boreholes 101-S02-MOD1 and 101-S09-MOD1 located in the Lac du Bonnet batholith near Pinawa, Manitoba. The purpose of the study is to ascertain if any anisotropy in terms of the uniaxial mechanical properties exists in the Lac du Bonnet samples and, if so, to what extent.

This represents the fourth in a series of reports to be published as data becomes available. A final report containing detailed analysis of the results will be written after all the sample suites have been tested.

---

\*Research Officer, Canadian Mine Technology Laboratory, Mining Research Laboratories, CANMET, Energy, Mines and Resources Canada, Ottawa, Ontario.

Keywords

Anisotropy, Rock Properties, Mechanical, Young's Modulus, Poisson's Ratio, Uniaxial Compressive Strength, Velocity, Lac du Bonnet

i



c 2  
CPUB

# ÉTUDE DES PROPRIÉTÉS ANISOTROPES DE SPÉCIMEN DE GRANITE DE LAC DU BONNET: RAPPORT #4

par

Rand Jackson\*

## RÉSUMÉ

Dans le but de déterminer le degré d'anisotropie dans les propriétés mécaniques de spécimens de granite de Lac du Bonnet, on a mesuré la vitesse ainsi que la résistance à la compression uniaxiale d'échantillons prélevés dans les trous de sonde 101-S02-MOD1 et 101-S09-MOD1, situés près de Pinawa au Manitoba.

Ce rapport est le quatrième d'une série de rapports qui seront publiés au fur et à mesure que les résultats deviendront disponibles. Un rapport final renfermant un résumé de tous les résultats d'essais, y compris des analyses détaillées, sera préparé.

---

\*Agent de recherche, Laboratoire canadien de technologie minière, Laboratoires de recherche minière, CANMET, Énergie, Mines et Ressources Canada, Ottawa, Ontario.

### Termes-clés

anisotrope, propriétés mécaniques des roches, module de Young, rapport de Poisson, résistance à la compression uniaxiale, vitesse, Lac du Bonnet

# CONTENTS

	<u>Page No.</u>
ABSTRACT . . . . .	i
RÉSUMÉ . . . . .	ii
INTRODUCTION . . . . .	1
IDENTIFICATION OF SPECIMENS AND TESTS . . . . .	1
DESCRIPTION OF TEST MEASUREMENTS . . . . .	3
DATA TREATMENT . . . . .	3
DATA SUMMARY . . . . .	5
FAILURE CHARACTERISTICS . . . . .	7
ACKNOWLEDGEMENTS . . . . .	7
REFERENCES . . . . .	8
APPENDIX A . . . . .	23

## TABLES

1	Summary of Sample Depth, Dimensions, Density and Orientation . . . . .	2
2	Summary of Ultrasonic Velocity Properties . . . . .	5
3	Summary of Uniaxial Compression Properties . . . . .	6

## FIGURES

1	Axial and circumferential stress/strain curves for anisotropy specimens: Drill Hole 101-S09-MOD1, Depth = 3.489 m . . . . .	9
2	Axial and circumferential stress/strain curves for anisotropy specimens: Drill Hole 101-S09-MOD1, Depth = 4.190 m . . . . .	10
3	Axial and circumferential stress/strain curves for anisotropy specimens: Drill Hole 101-S09-MOD1, Depth = 4.240 m . . . . .	11
4	Axial and circumferential stress/strain curves for anisotropy specimens: Drill Hole 101-S09-MOD1, Depth = 4.290 m . . . . .	12
5	Axial and circumferential stress/strain curves for anisotropy specimens: Drill Hole 101-S09-MOD1, Depth = 3.340 m . . . . .	13
6	Axial and circumferential stress/strain curves for anisotropy specimens: Drill Hole 101-S09-MOD1, Depth = 3.580 m . . . . .	14

7	Axial and circumferential stress/strain curves for anisotropy specimens: Drill Hole 101-S09-MOD1, Depth = 3.719 m . . . .	15
8	Axial and circumferential stress/strain curves for anisotropy specimens: Drill Hole 101-S09-MOD1, Depth = 3.955 m . . . .	16
9	Axial and circumferential stress/strain curves for anisotropy specimens: Drill Hole 101-S09-MOD1, Depth = 4.054 m . . . .	17
10	Axial and circumferential stress/strain curves for anisotropy specimens: Drill Hole 101-S02-MOD1, Depth = 0.746 m . . . .	18
11	Axial and circumferential stress/strain curves for anisotropy specimens: Drill Hole 101-S02-MOD1, Depth = 1.320 m . . . .	19
12	Axial and circumferential stress/strain curves for anisotropy specimens: Drill Hole 101-S02-MOD1, Depth = 1.250 m . . . .	20
13	Axial and circumferential stress/strain curves for anisotropy specimens: Drill Hole 101-S02-MOD1, Depth = 1.170 m . . . .	21
14	Axial and circumferential stress/strain curves for anisotropy specimens: Drill Hole 101-S02-MOD1, Depth = 1.045 m . . . .	22

## INTRODUCTION

As part of the Canadian Nuclear Fuel Waste Management Project, Atomic Energy of Canada Limited is characterizing various rock formations to determine their suitability for long term disposal of high level wastes. The program also includes the construction of an underground research laboratory (URL) near Pinawa, Manitoba to provide an opportunity for extensive in situ investigations.

Biaxial testing conducted on core obtained during the construction phase of the URL has indicated that the rock may be anisotropic in terms of modulus of elasticity, (1). It was felt that further study in the form of acoustic velocity and uniaxial compression testing could provide additional insight into this behaviour.

This represents the fourth in a series of reports which were published as sample suites were tested and data became available. A fifth and final report will follow which will include a detailed examination and analysis of the results.

## IDENTIFICATION OF SPECIMENS AND TESTS

Fourteen samples were used for this test series; 9 from drill hole 101-S09-MOD1 and 5 from borehole 101-S02-MOD1. The location and orientation of the drill holes can be found in Appendix A and are summarized below;

101-S09-MOD1:	Collar coordinates:	N 5,570,466.087
		E 295,785.878
		elev. 160.250
	Orientation:	plunge = $-03.22^\circ$ (up)
		trend (direction) = $111.07^\circ$
101-S02-MOD1:	Collar coordinates:	N 5,570,475.061
		E 295,789.119
		elev. 160.580
	Orientation:	plunge = $-2.89^\circ$ (up)
		trend (direction) = $026.80^\circ$

The 45 mm. diameter test specimens were prepared by recoring 200 mm. diameter cores obtained from drill holes along orthogonal axes. The specimens were then identified according to their location and orientation as follows;

A: depth of the collar of the 45 mm hole from the collar of the 200 mm hole



B: angle  $\beta$  gives the location of the collar of the 45 mm hole around the circumference of the 200 mm core. The angle is measured clock-wise (looking down hole) from the orientation mark on the top of the core.

C: angle  $\alpha$  is the angle between the core axis of the 45 mm core and the 200 mm core. The angle is measured clockwise (ie. dip) from the down hole direction of the 200 mm core.

Table 1 provides a summary of the specimen depth, dimensions, density and orientation. The following properties were determined for the samples listed;

- 1) compressive wave velocity
- 2) shear wave velocity
- 3) dynamic shear modulus,  $G_d$
- 4) dynamic Young's modulus,  $E_d$
- 5) Poisson's ratio (determined using velocity data)
- 6) uniaxial compressive strength
- 7) Poisson's ratio
- 8) tangent modulus of elasticity,  $E_t$
- 9) secant modulus of elasticity,  $E_s$

Table 1 - Summary of sample depth, dimensions, density and orientation

Drill Hole	Sample Depth (m)	Length (mm)	Diameter (mm)	Density (gm/cc)	$\alpha$	$\beta$
101-S09-MOD1	3.489	103.88	44.46	2.70	0°	<i>axial</i>
	4.190	104.28	44.42	2.98	90°	0°
	4.240	105.04	44.30	3.05	90°	30°
	4.290	104.44	44.32	2.70	90°	60°
	4.340	104.42	44.42	2.71	90°	90°
	3.580	105.14	44.22	2.62	30°	0°
	3.719	104.48	44.10	3.14	30°	90°
	3.955	104.38	44.30	2.90	60°	0°
	4.054	104.82	44.40	2.74	60°	90°
101-S02-MOD1	0.746	104.92	44.34	2.63	0°	<i>axial</i>
	1.320	104.50	44.40	2.63	90°	0°
	1.250	105.32	44.38	2.63	90°	30°
	1.170	105.24	44.42	2.63	90°	60°
	1.045	99.68	44.42	2.63	90°	90°

## DESCRIPTION OF TEST MEASUREMENTS

Compression and shear\* wave velocity measurements were carried out on samples prior to being gauged for elastic deformation measurement. The testing equipment consisted of: transmitting and receiving platens containing piezoelectric transducers, a high voltage pulse generator, a signal amplifier and a Tektronix Type 555 dual beam oscilloscope equipped with delay sweep and a time base resolution of 0.01 micro-seconds. The zero time delay was determined by measuring the time of wave arrival across three steel samples of different lengths. These arrival times could then be extrapolated to correspond to a specimen of zero length.

For an outline of the uniaxial compression procedure, the reader is referred to Technical Data 303410-M01/78 (2). The two Phillips PR 9302 strain bridges and the Mosely Autograph 2FRA X-Y recorder referred to in that document were replaced, in the present study, by two Bruel and Kjaer Type 1526 strain indicators and a Hewlett Packard 7046B X-Y recorder. These equipment were used to measure and record the axial and transverse strains as a function of axial load. Linear variable differential transducers (LVDT's) were also utilized to provide redundant measurements of axial deformation.

## DATA TREATMENT

The compressional and shear wave velocities were determined by dividing the specimen length by the wave travel time through the specimen. The dynamic properties were, then, calculated using the following equations (4);

Dynamic Young's Modulus†

$$E_d = \frac{\rho V_s^2 (3V_p^2 - 4V_s^2)}{V_p^2 - V_s^2} \quad (1)$$

where;  $E_d$  =dynamic Young's modulus

$V_s$  =shear wave velocity

$V_p$  =compressional wave velocity

$\rho$  =density

---

\* Due to equipment failure, shear wave velocity measurements could not be conducted on borehole 101-S09-MOD1 specimens.

† Used when shear wave velocity measurements were available.

### Dynamic Young's Modulus\*

$$E_d = \frac{V_p^2 \rho (1 + \nu)(1 - \nu)}{(1 - \nu)} \quad (2)$$

where;  $E_d$  =dynamic Young's modulus  
 $V_p$  =compressional wave velocity  
 $\rho$  =density  
 $\nu$  =Poisson's ratio=.25

### Dynamic Shear Modulus

$$G_d = \rho V_s^2 \quad (3)$$

where;  $G_d$  =dynamic shear modulus  
 $V_s$  =shear wave velocity  
 $\rho$  =density

### Poisson's Ratio (based on velocity data)

$$\nu_d = \frac{V_p^2 - 2V_s^2}{2(V_p^2 - V_s^2)} \quad (4)$$

where;  $\nu_d$  =Poisson's ratio  
 $V_s$  =shear wave velocity  
 $V_p$  =compressional wave velocity

The stress-strain curves were computer generated using analog outputs from the strain bridges and press. The tangent modulus of elasticity ( $E_t$ ) was calculated for each sample by determining the slope of the tangent to the axial strain curve at 50% of the failure load. The secant modulus of elasticity ( $E_s$ ) was calculated by determining the slope of the line joining the origin to the point on the axial strain curve corresponding to 50% of the failure load. The ultimate compressive strength of each sample was calculated by dividing the sample failure load by the sample's cross-sectional area. The ratio of the tangent to the axial strain curve to the tangent to the transverse strain curve at 50% failure load was used to determine the sample's Poisson's ratio ( $\nu$ ). Please note that the curves for samples 1.250 and 1.320 from borehole 101-S02-MOD1 are incomplete due to the failure of the strain gauges prior to the ultimate strength being achieved. However, sufficient data was available to determine the moduli values at 50% of the failure load.

---

\* Used when shear wave velocity measurements were not available.

## DATA SUMMARY

Table 2 contains the results of the ultrasonic velocity measurements including the calculated values of the dynamic shear modulus, dynamic Young's modulus as well as Poisson's ratio estimated on the basis of velocity data for each sample. As noted in Table 2, an estimated Poisson's ratio of .25 was used in calculating the dynamic Young's moduli for borehole 101-S09-MOD1. This, as well as the inability to calculate the dynamic shear moduli for these samples, is due to a lack of shear wave velocity data.

Table 3 summarizes the uniaxial compression measurements which include loading rate, uniaxial compressive strength, tangent modulus of elasticity, secant modulus of elasticity, Poisson's ratio and the predominant mode of failure for each specimen.

Figures 1 through 14 represent the circumferential and axial stress/strain curves for each sample. Also included on the figures is a summary of the sample's depth, orientation, tangent modulus and Poisson's ratio.

Table 2 - Summary of ultrasonic velocity properties

Drill hole	Sample depth (m)	P-wave velocity (km/sec)	S-wave velocity (km/sec)	Dynamic shear modulus, $G_d$ (GPa)	Dynamic Young's modulus, $E_d$ (GPa)	Poisson's ratio*
101-S09-MOD1	3.489	5.14	3.55	N/A	59.49	0.25
	4.190	5.03	3.76	N/A	62.91	0.25
	4.240	4.38	3.91	N/A	48.79	0.25
	4.290	4.23	4.00	N/A	40.21	0.25
	4.340	3.94	3.76	N/A	35.02	0.25
	3.580	4.06	3.56	N/A	36.11	0.25
	3.719	4.25	4.00	N/A	47.18	0.25
	3.955	5.04	4.04	N/A	61.16	0.25
	4.054	4.46	3.89	N/A	45.27	0.25
101-S02-MOD1	0.746	5.22	3.48	31.89	70.15	0.10
	1.320	5.87	3.72	36.31	84.63	0.16
	1.250	5.71	3.65	35.02	80.87	0.15
	1.170	4.91	3.33	29.20	62.72	0.07
	1.045	4.27	2.86	21.47	46.95	0.09

\*.25 was used as an estimate of Poisson's ratio for determining  $E_d$  for borehole 101-S09-MOD1

Table 3 - Summary of uniaxial compression properties

Drill hole	Sample depth (m)	Loading rate (MPa/sec)	Uniaxial compressive strength (MPa)	Tangent modulus of elasticity (GPa)	Secant modulus of elasticity (GPa)	Poisson's ratio	Predominant failure characteristic
101-S09-MOD1	3.489	0.75	133	73.90	60.69	0.20	axial splitting
	4.190	0.75	213	99.45	103.50	0.22	axial splitting
	4.240	0.75	232	107.8	113.70	0.80	axial splitting
	4.290	0.75	206	83.29	79.41	0.25	axial splitting
	4.340	0.75	163	76.71	67.09	0.23	axial splitting
	3.580	0.75	165	72.62	56.08	0.22	axial splitting
	3.719	0.75	158	84.83	98.09	0.20	axial splitting
	3.955	0.75	188	74.98	72.71	0.19	diagonal plane
	4.054	0.75	198	71.57	65.25	0.22	axial splitting
101-S02-MOD1	0.746	0.75	152	69.45	59.03	0.23	diagonal plane
	1.320	0.75	156	76.47	72.84	0.34	axial splitting
	1.250	0.75	141	70.01	66.28	0.20	axial splitting
	1.170	0.75	164	72.41	59.13	0.25	axial splitting
	1.045	0.75	190	68.20	53.84	0.19	axial splitting

## FAILURE CHARACTERISTICS

The predominant mode of failure was that of axial splitting and slabbing. Partially formed single diagonal failure planes were also apparent in two samples although the explosive nature of the failures made it impossible to measure failure angles.

## ACKNOWLEDGEMENTS

The author would like to acknowledge the valuable assistance of Mr. Milan Situm during this test program.

## REFERENCES

1. Lang, P., "Personal communication", 1985.
2. Annor, A. and Geller, L., "Dilatational velocity, Young's modulus, Poisson's ratio, uniaxial compressive strength and Brazilian tensile strength for WN1 and WN2 samples", CANMET/MRL Technical Data 303410-M01/78, 1978.
3. Lama, R.D., Saluja, S.S., Vutikuri, V.S., "Handbook on mechanical properties of rocks", Volume II, Chapter 7, Trans Tech Publications.

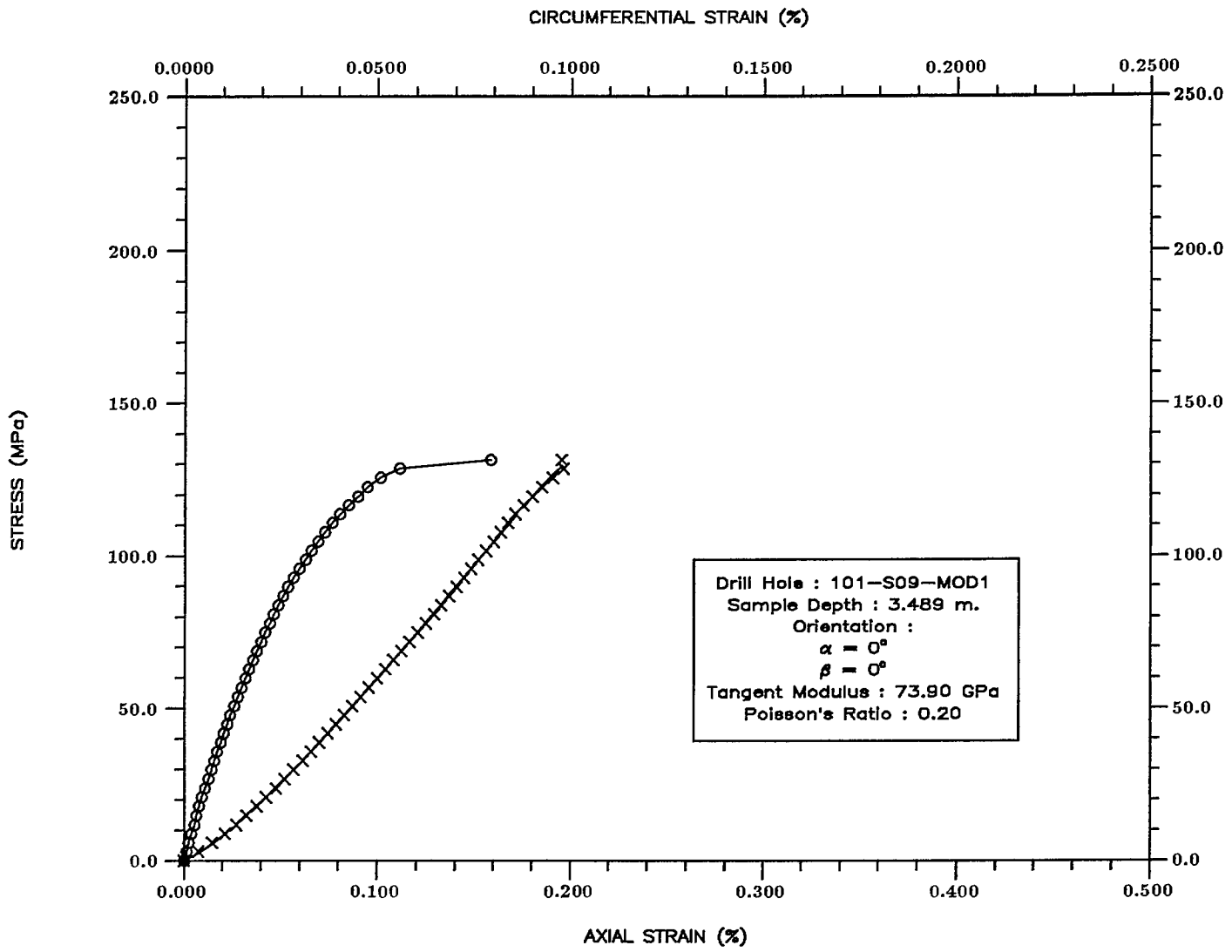


Fig. 1 : Axial and circumferential stress/strain curves for anisotropy test specimens.



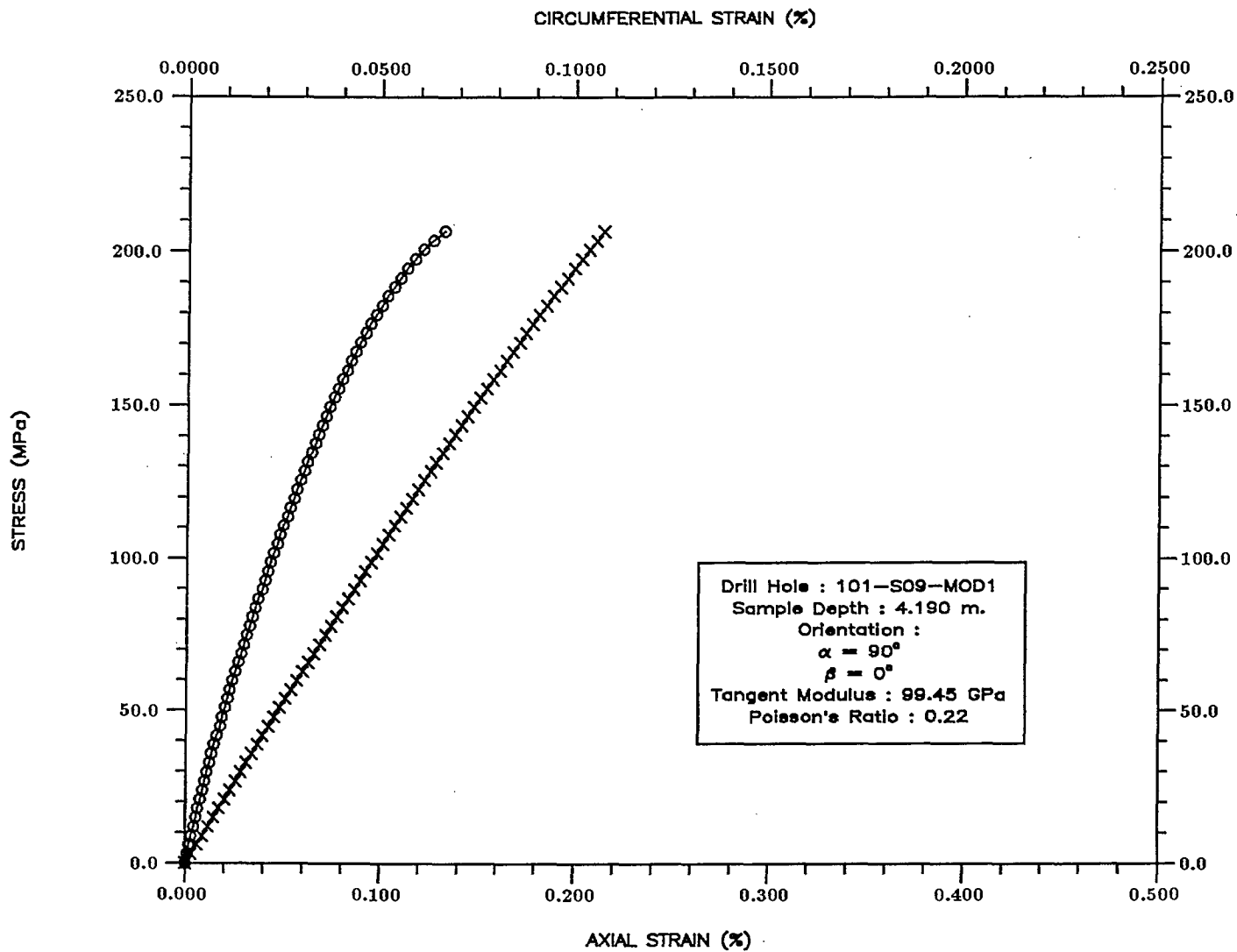


Fig. 2 : Axial and circumferential stress/strain curves for anisotropy test specimens.

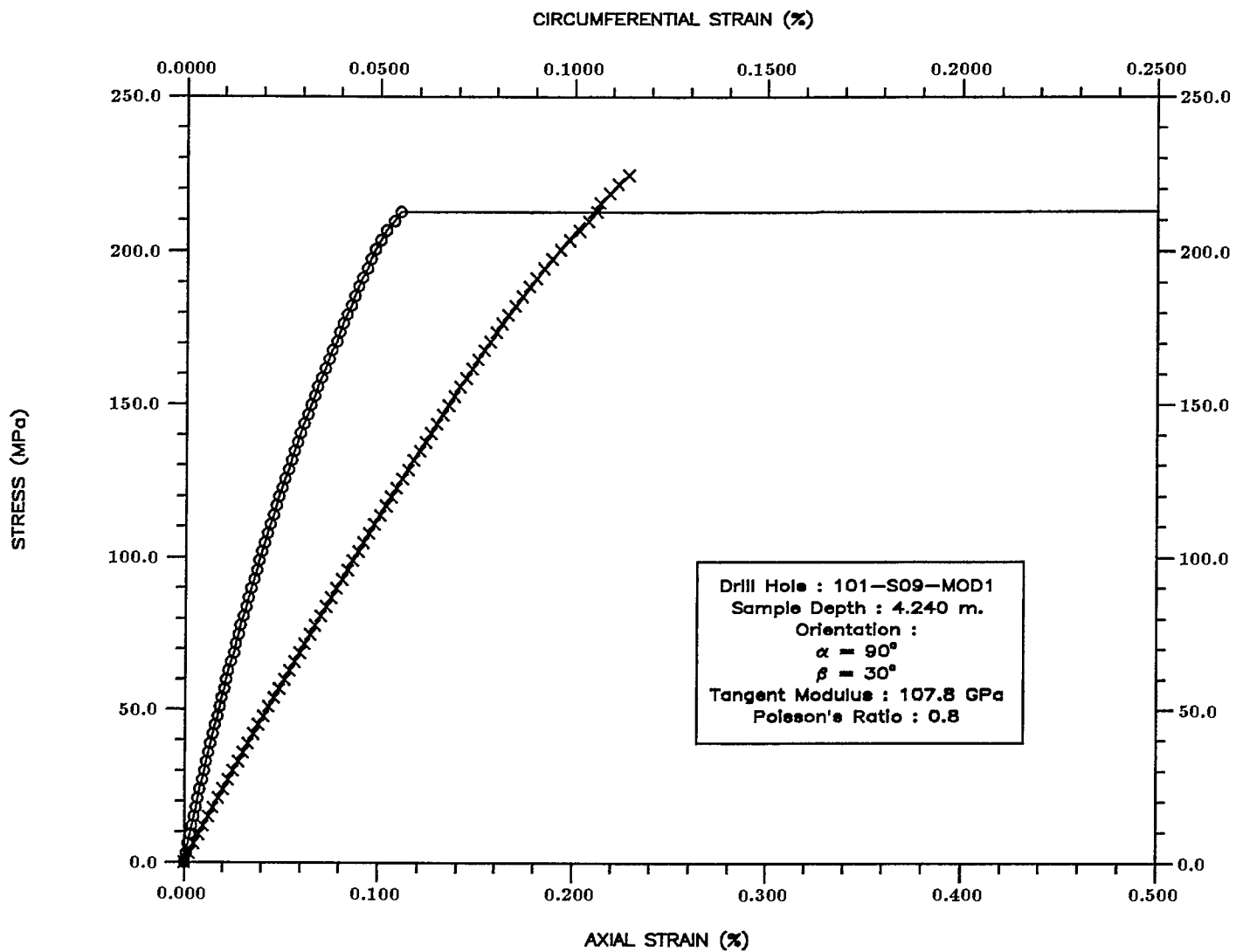


Fig. 3 : Axial and circumferential stress/strain curves for anisotropy test specimens.

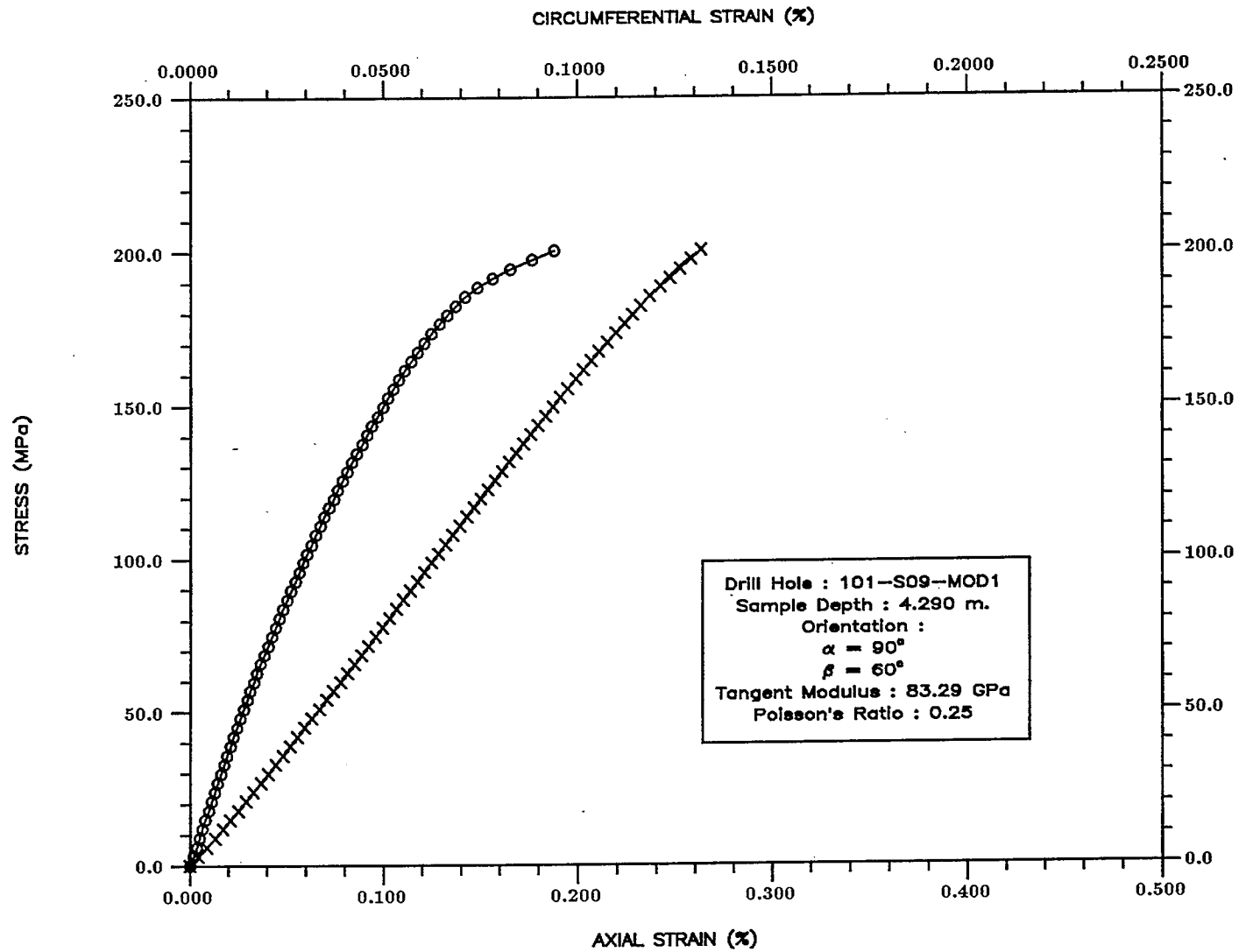


Fig. 4 : Axial and circumferential stress/strain curves for anisotropy test specimens.

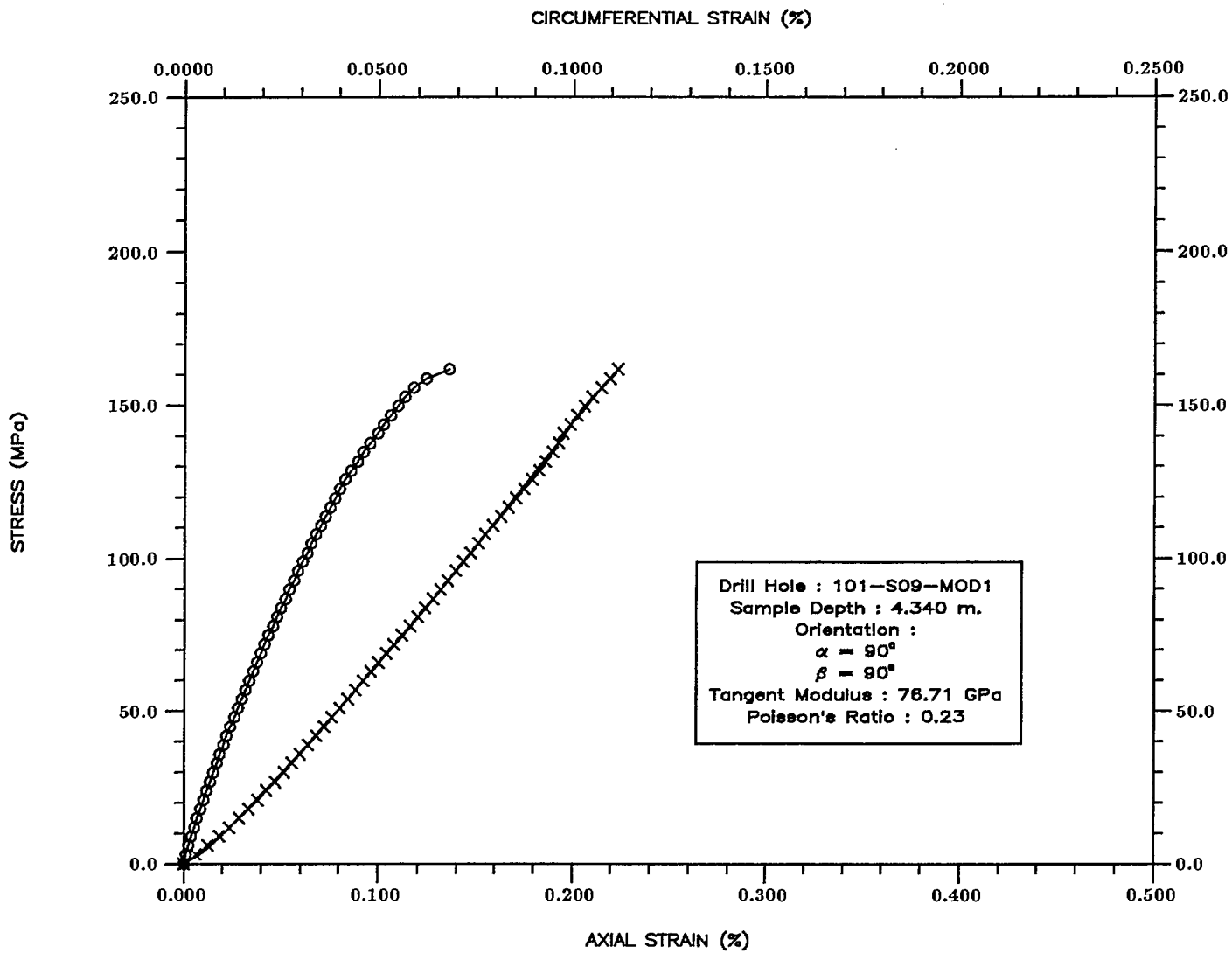


Fig. 5 : Axial and circumferential stress/strain curves for anisotropy test specimens.

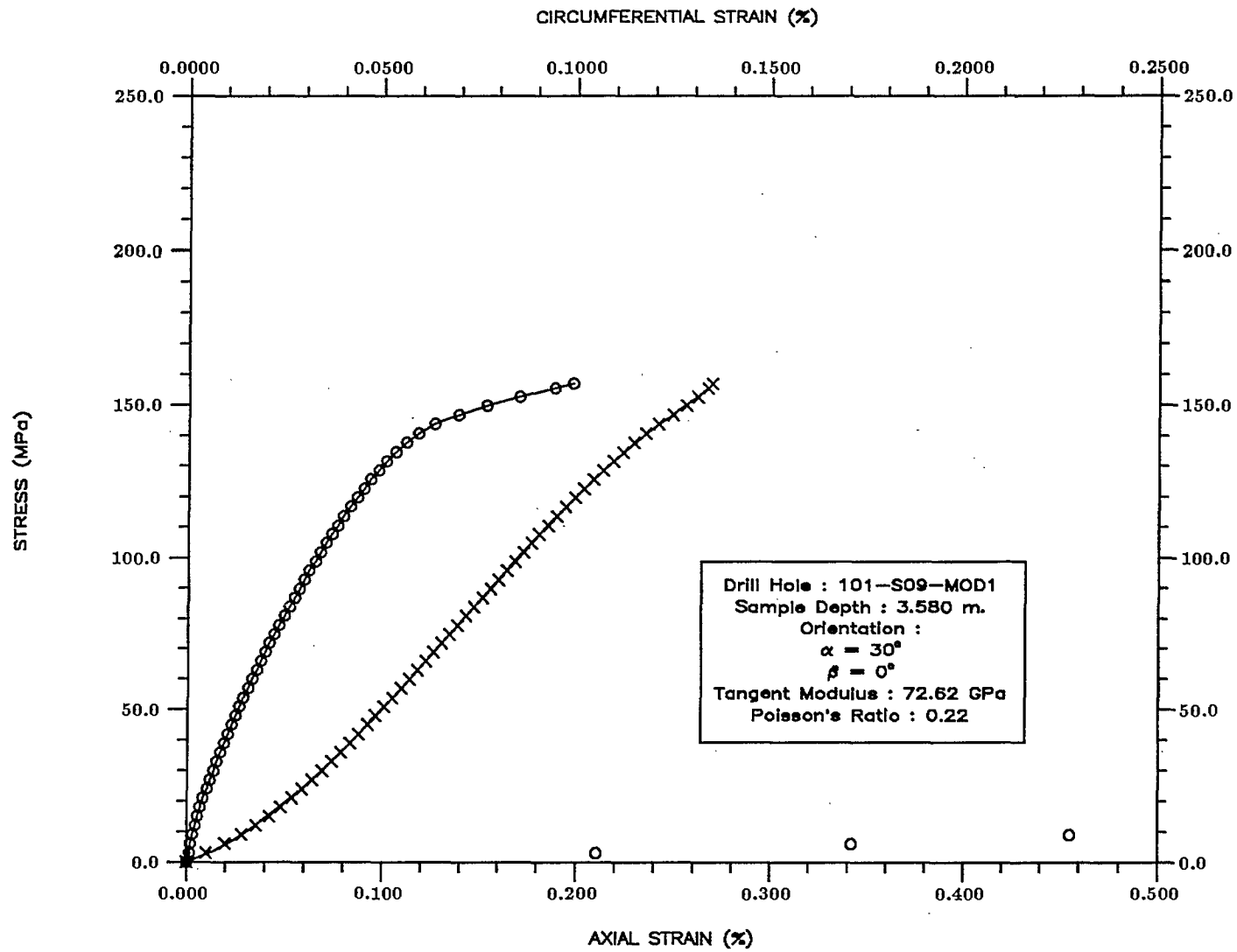


Fig. 6 : Axial and circumferential stress/strain curves for anisotropy test specimens.

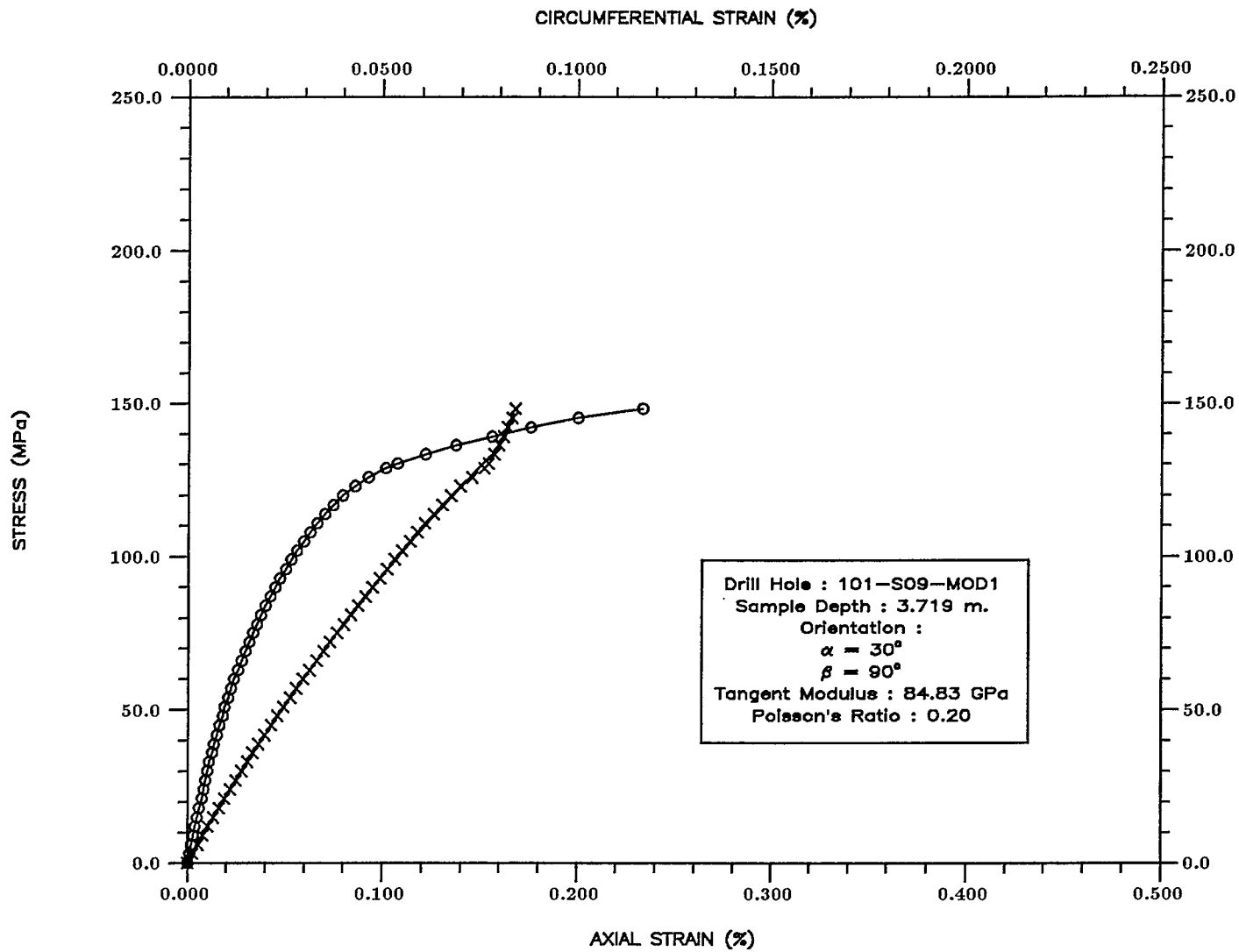


Fig. 7 : Axial and circumferential stress/strain curves for anisotropy test specimens.

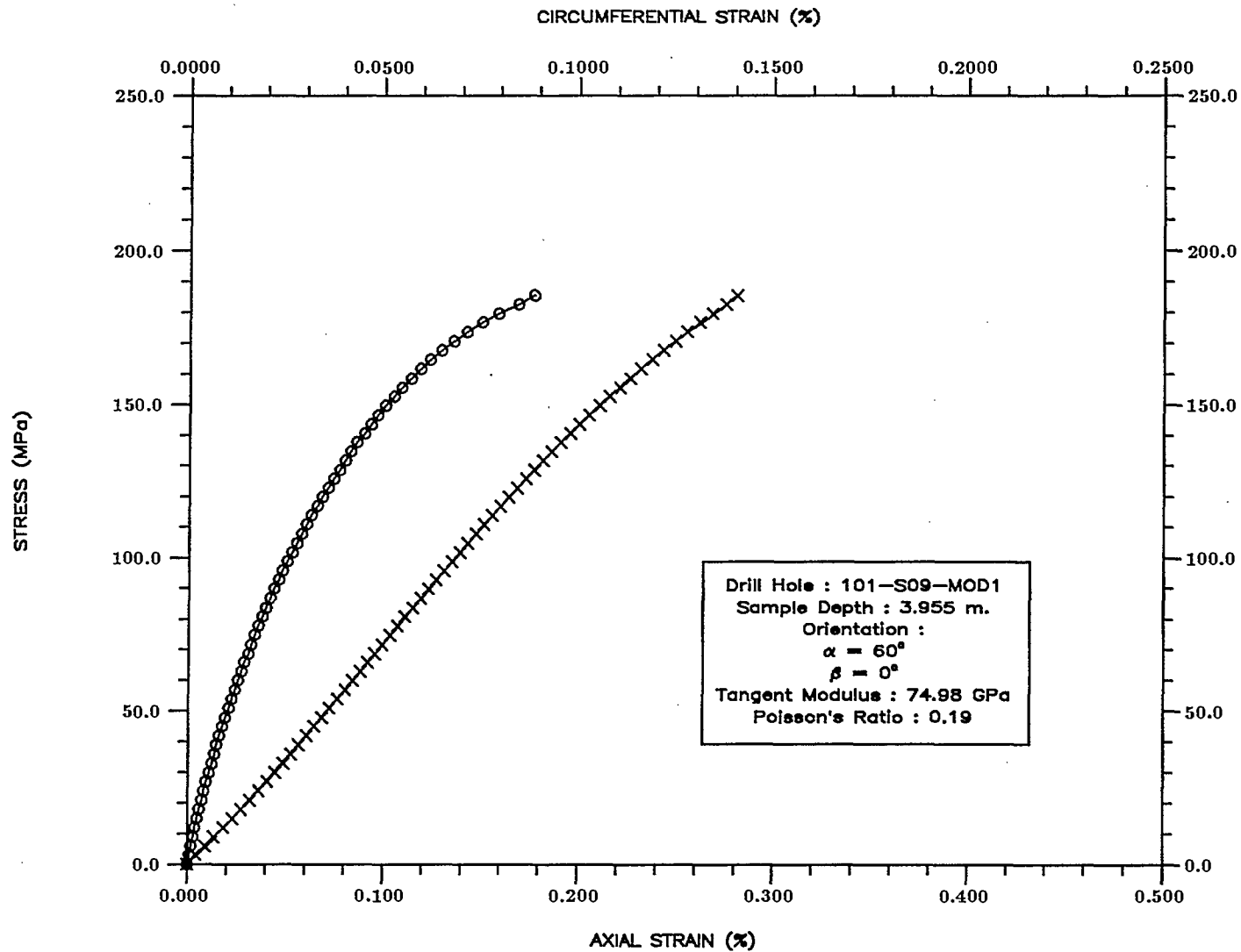


Fig. 8 : Axial and circumferential stress/strain curves for anisotropy test specimens.

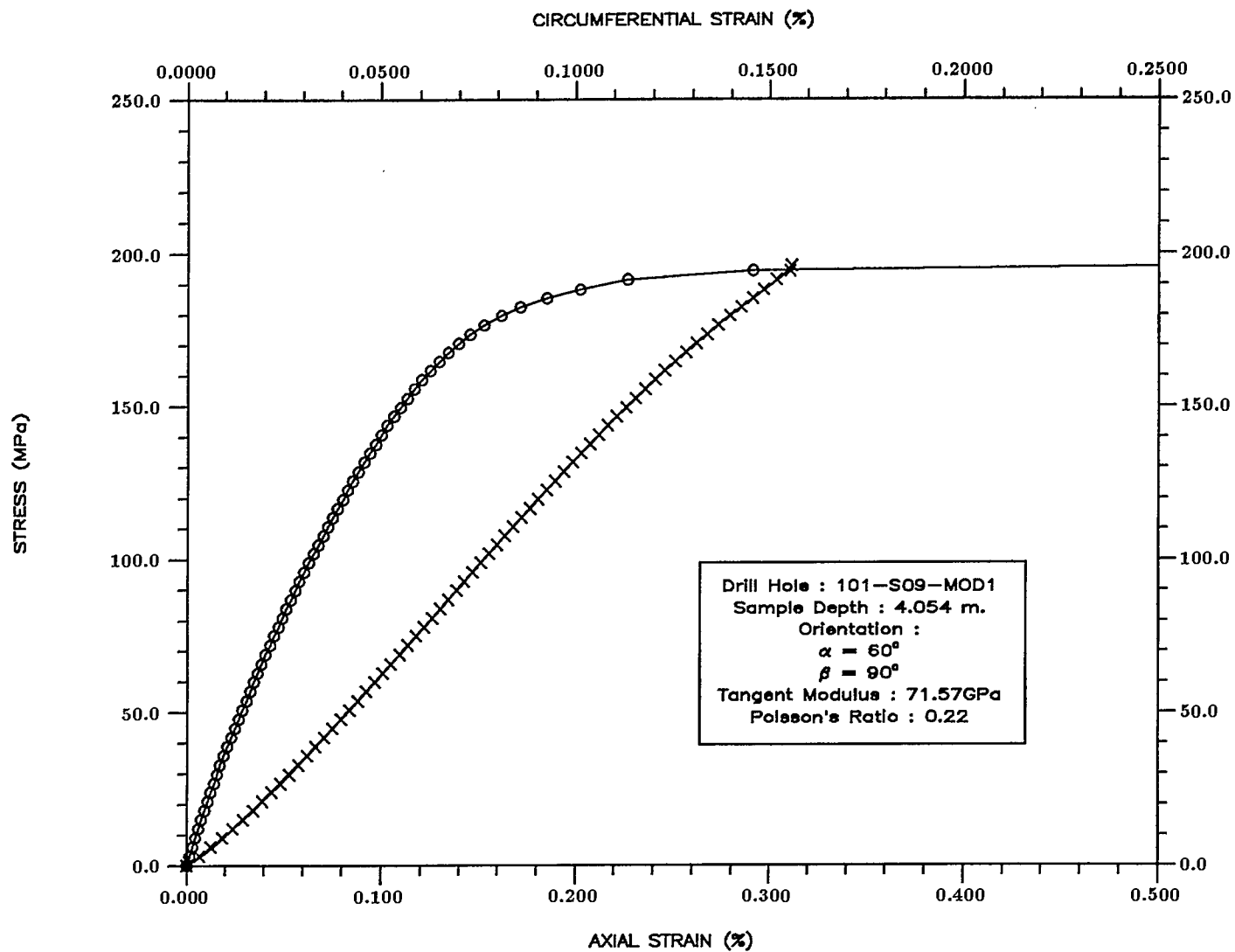


Fig. 9 : Axial and circumferential stress/strain curves for anisotropy test specimens.



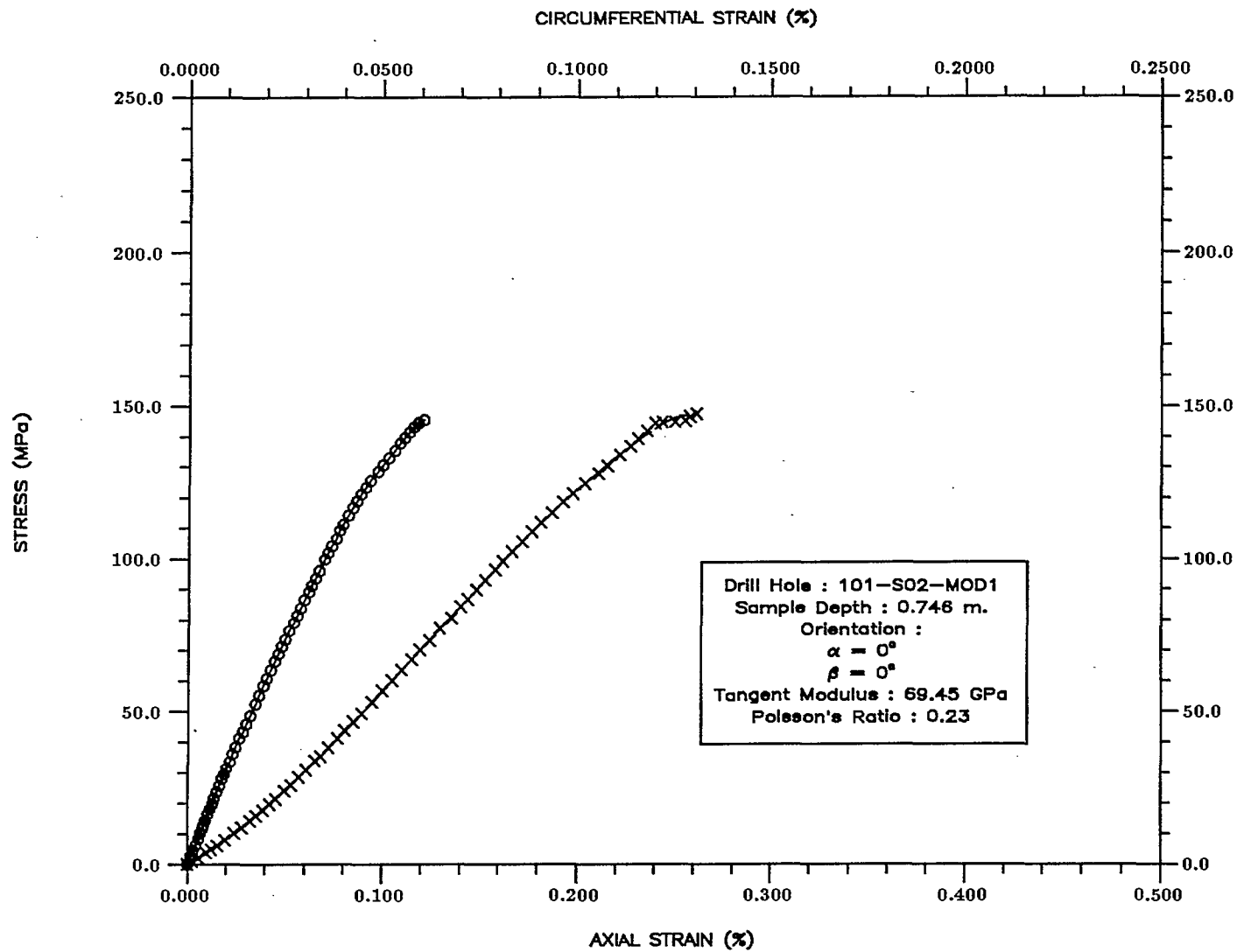


Fig. 10 : Axial and circumferential stress/strain curves for anisotropy test specimens.

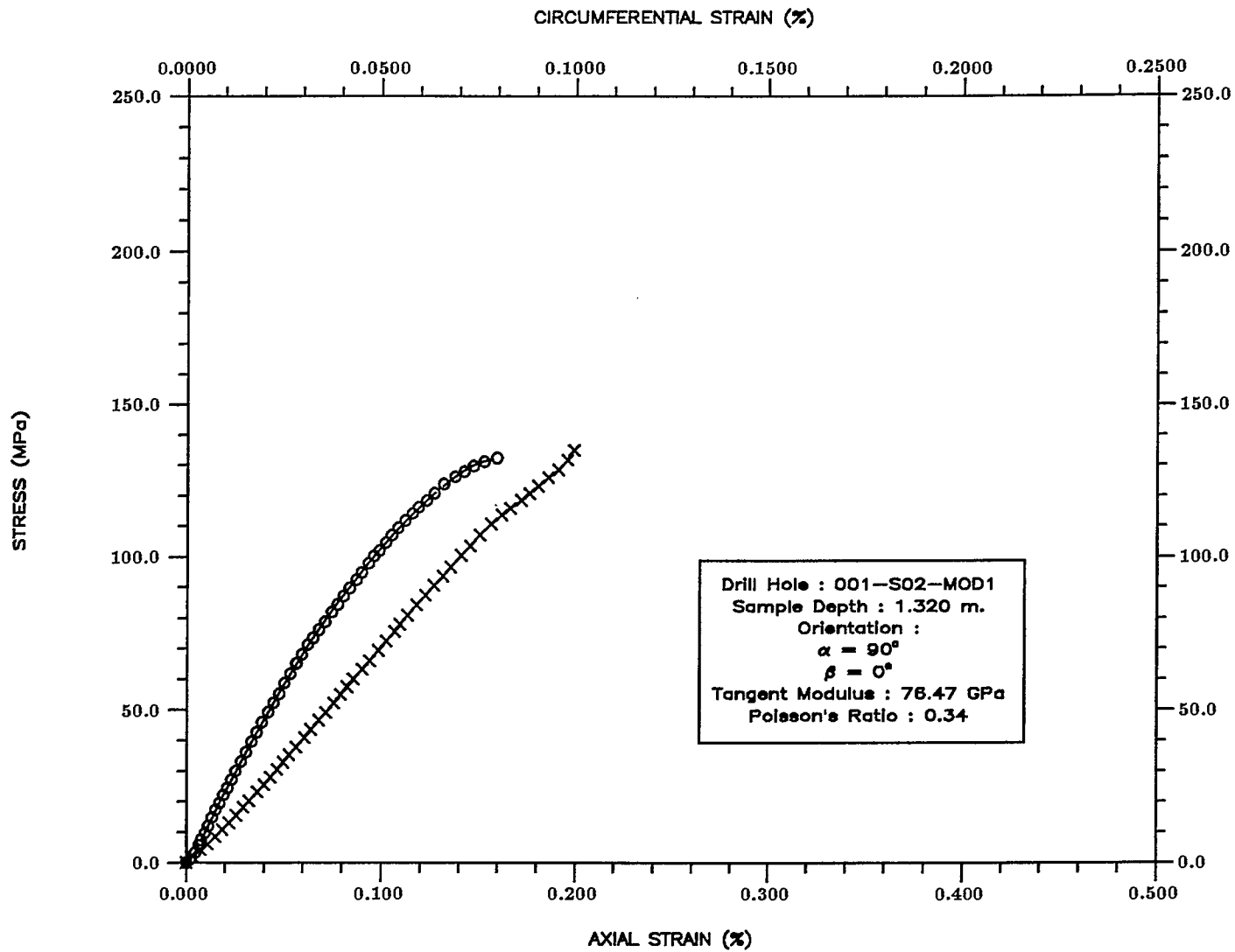


Fig. II : Axial and circumferential stress/strain curves for anisotropy test specimens.

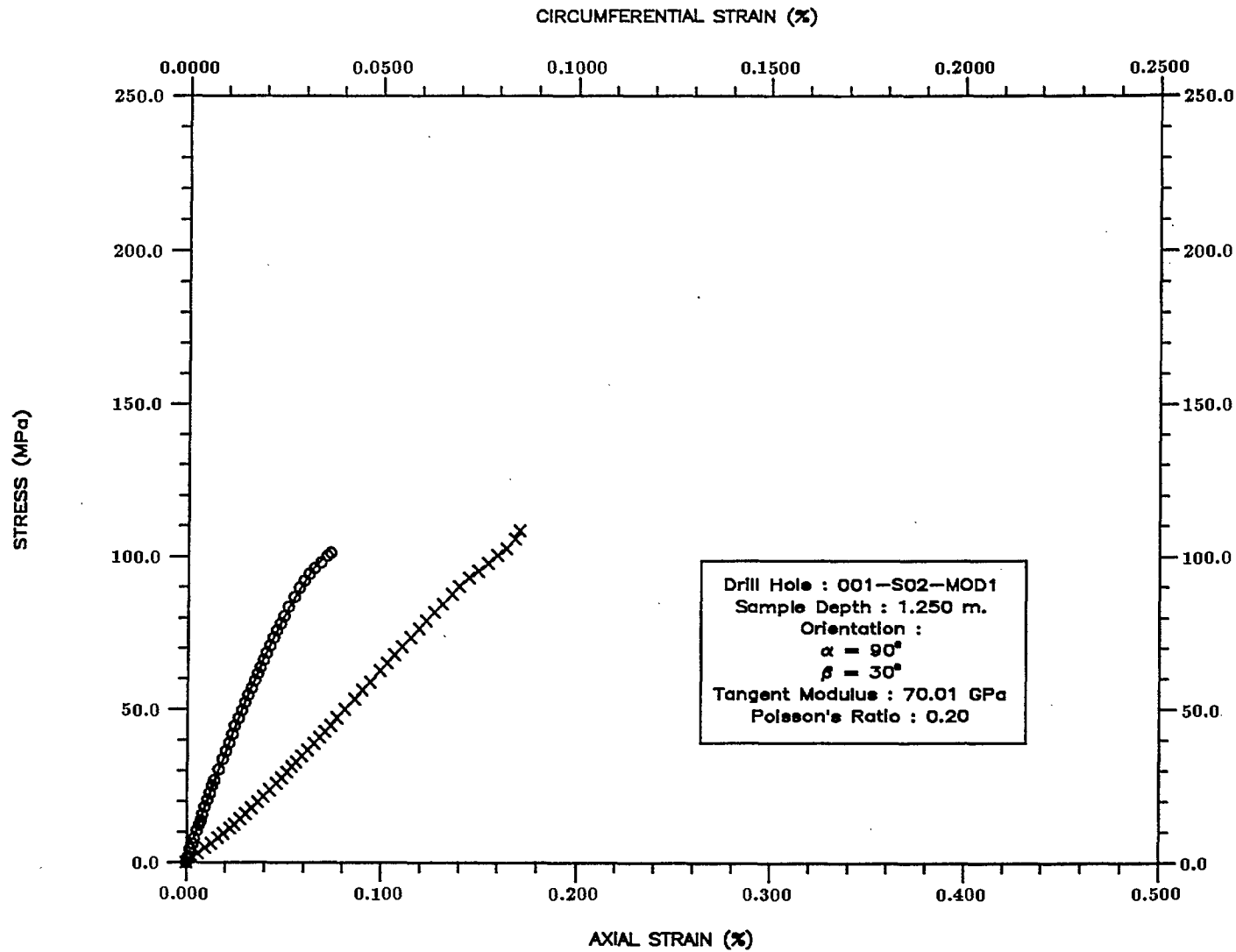


Fig. 12 : Axial and circumferential stress/strain curves for anisotropy test specimens.

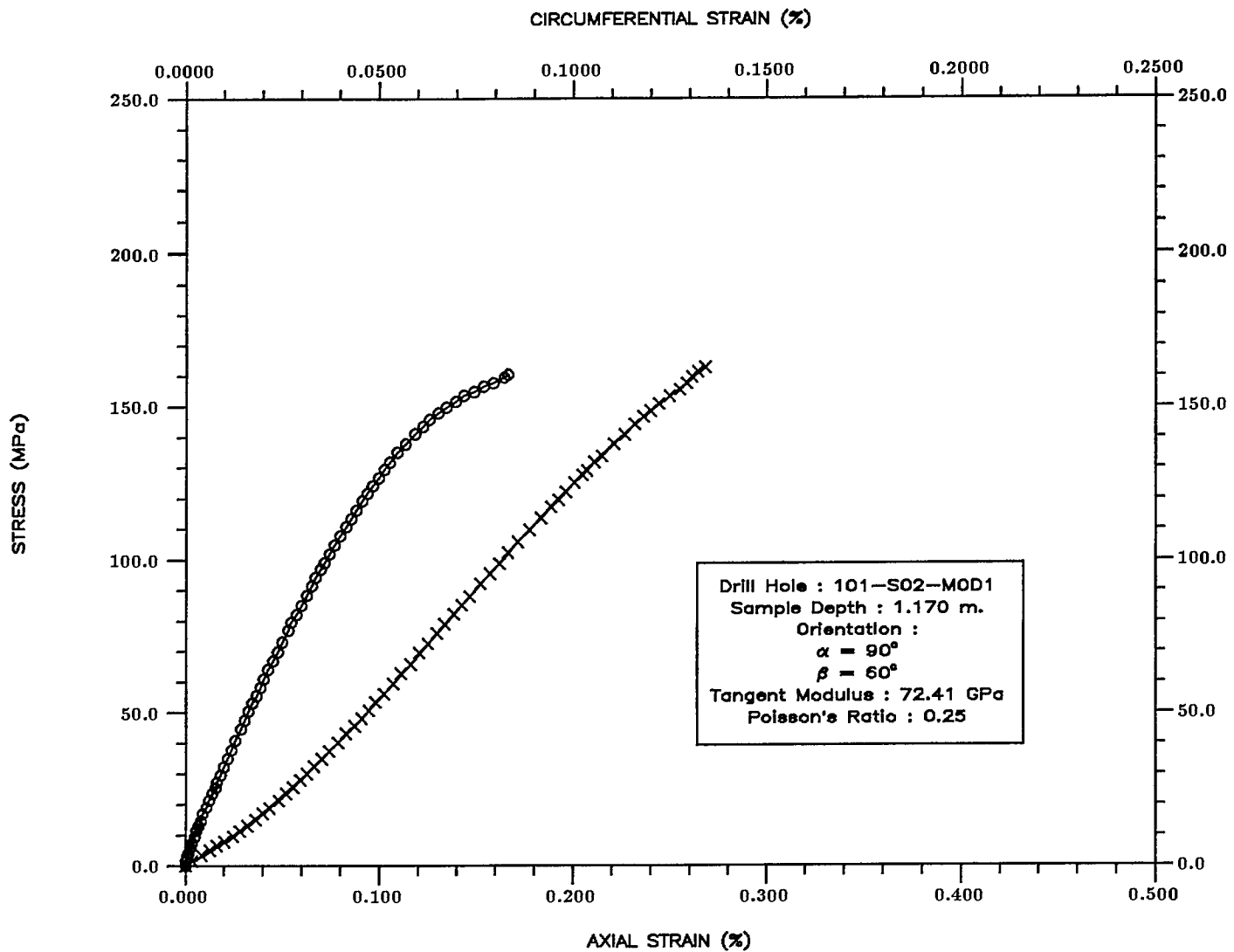


Fig. 13 : Axial and circumferential stress/strain curves for anisotropy test specimens.

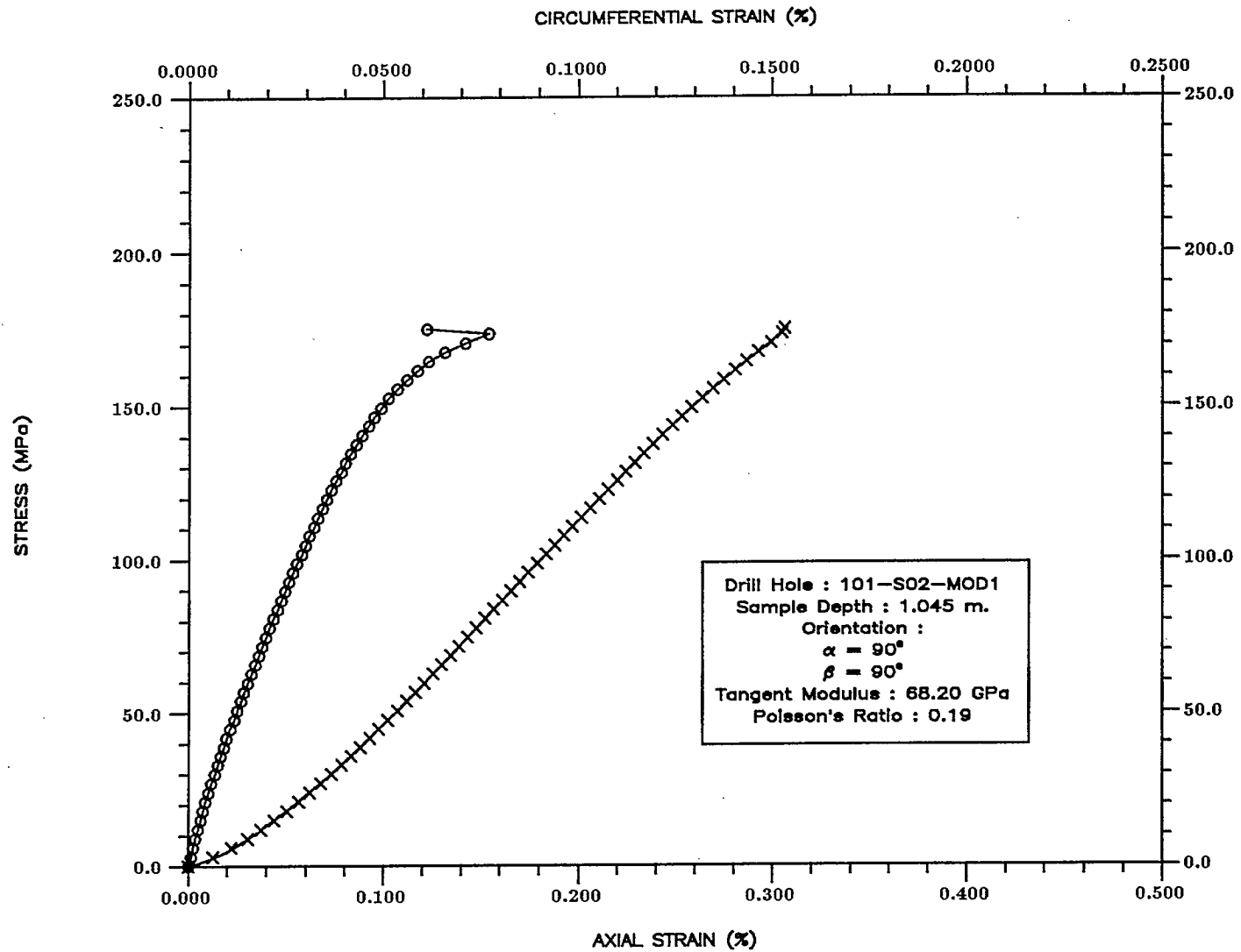


Fig. 14 : Axial and circumferential stress/strain curves for anisotropy test specimens.

# APPENDIX A



WASTE MANAGEMENT  
Atomic Energy of Canada Limited  
Research Company  
Pinawa, Manitoba, Canada  
ROE 1LO

GESTION DES DÉCHETS  
L'Énergie Atomique du Canada, Limitée  
Société de recherche

Tel (204) 753-2311

Telex 07-57553

Geological and Environmental Science Division  
Science de la terre et de l'environnement

1987 July 09

G-5410  
GSEB-87-268

Mr. Alfred Annor  
CANMET  
555 Booth Street  
Ottawa, Ontario  
K1A 0G1

Dear Mr. Annor:

The fifth batch of anisotropic properties samples will be sent to you this week. This batch consists of 15 samples from three 200 mm cores from drill hole numbers 101-S09-MOD1 and 101-S02-MOD1.

The attachments give the details of the 200 mm drill hole locations, the system for describing the 45 mm core location and orientation, and photographs of the samples. The sampling method was described in the previous correspondence.

If you have any questions, please call me at (204) 345-8625.

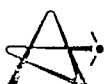
Yours truly,

Dwayne Onagi  
Geotechnical Science and  
Engineering Branch

D0/djs

Attachments

cc P.M. Thompson  
G.R. Simmons  
S.H. Whitaker  
P.A. Lang



DESIGNATION OF ANISOTROPIC PROPERTIES SAMPLES

The location and orientation of the 200 mm diameter core hole numbers are as follows:

101-S09-MOD1  
Collar Coordinates: N 5,570,466.087  
E 295,785.878  
elev. 160.250  
Orientation: Plunge (dip): -03.22° (up)  
Trend (direction): 111.07°

101-S02-MOD1  
collar coordinates: N 5,570,475.061  
E 295,789.119  
elev. 160.580  
Orientation: Plunge (dip): -02.89° (up)  
Trend (direction): 026.80°

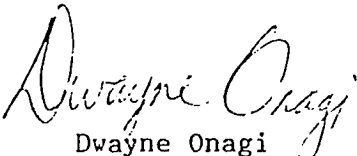
The location and orientation of the 45 mm cores taken from the 200 mm cores are defined as follows:

- a) depth of the collar of the 45 mm holes from the collar of the 200 mm hole.
- b) angle  $\beta$  gives the location of the collar of the 45 mm hole around the circumference of the 200 mm core. The angle is measured clockwise (looking down hole) from the orientation mark on the top of the 200 mm core (Figure 3).
- c) angle  $\alpha$  is the angle between the core axis of the 45 mm core and the 200 mm core. The angle is measured clockwise from the down hole direction of the 200 mm core (Figure 2).

The  $\alpha$  and  $\beta$  angles as well as the depth are marked on each core as well as on waterproof paper attached to each core. They are also listed in Tables 1 and 2.

In addition to these markings, there are two lines, an arrow, and  $\beta$  angle on the collar end of each 45 mm core (except the axial core) (Figure 1). One line indicates the axial direction of the 200 mm core and the arrow points down hole. The short line across the axial line indicates the point at which the depth is measured. The 45 mm core that is parallel to the 200 mm core axis, contains the axial line and arrow marked along the top of the core. Pieces of core that are not suitable for testing are marked "Do Not Test".

One piece of 45 mm core obtained from hole number 101-S09-MOD1 was damaged by intersecting a previously drilled hole. It is labeled "Do not Use". Two other pieces of core from that hole were broken while drilling (Table 1). Two pieces of 45 mm core obtained from hole number 101-S02-MOD1 were broken while drilling as well (Table 2).

  
Dwayne Onagi  
1987 July 09



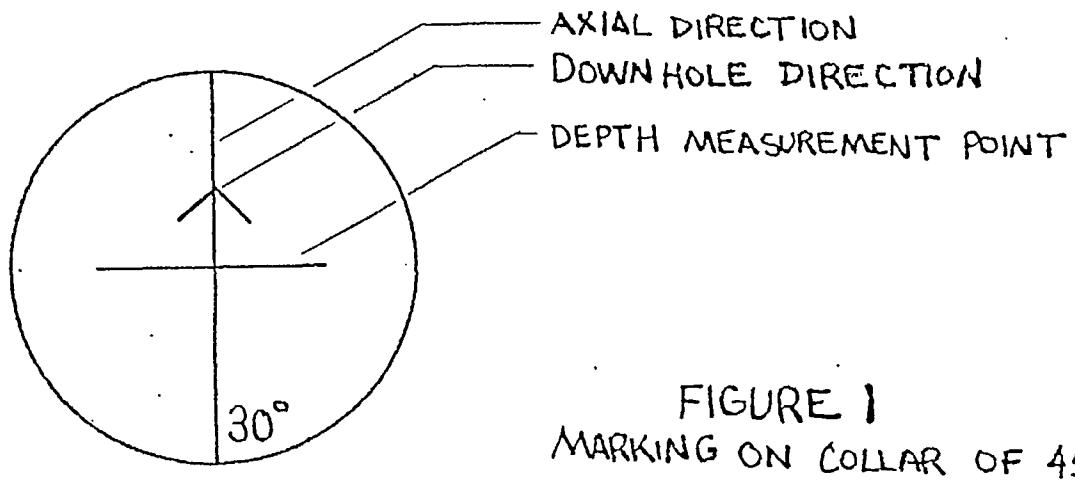


FIGURE 1  
MARKING ON COLLAR OF 45 MM CORE

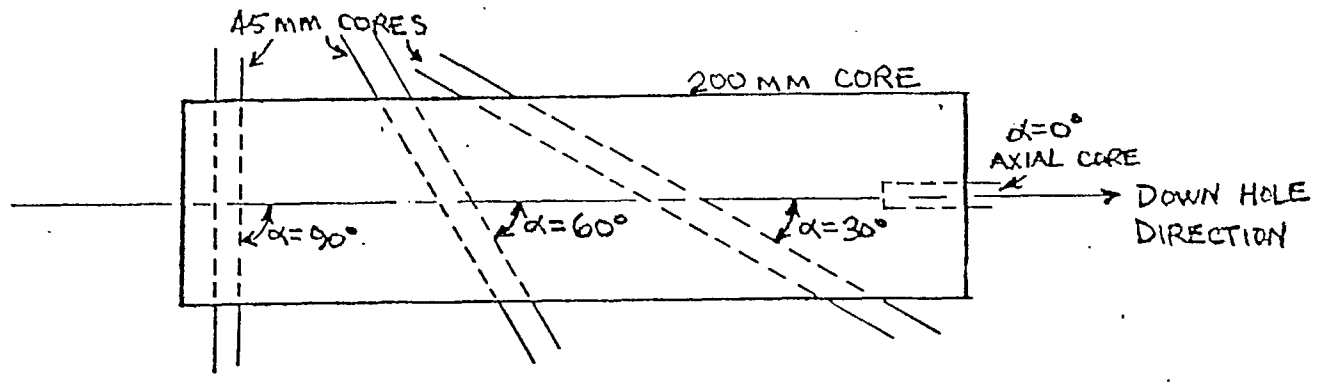


FIGURE 2  
 $\alpha$  ANGLE DESIGNATION

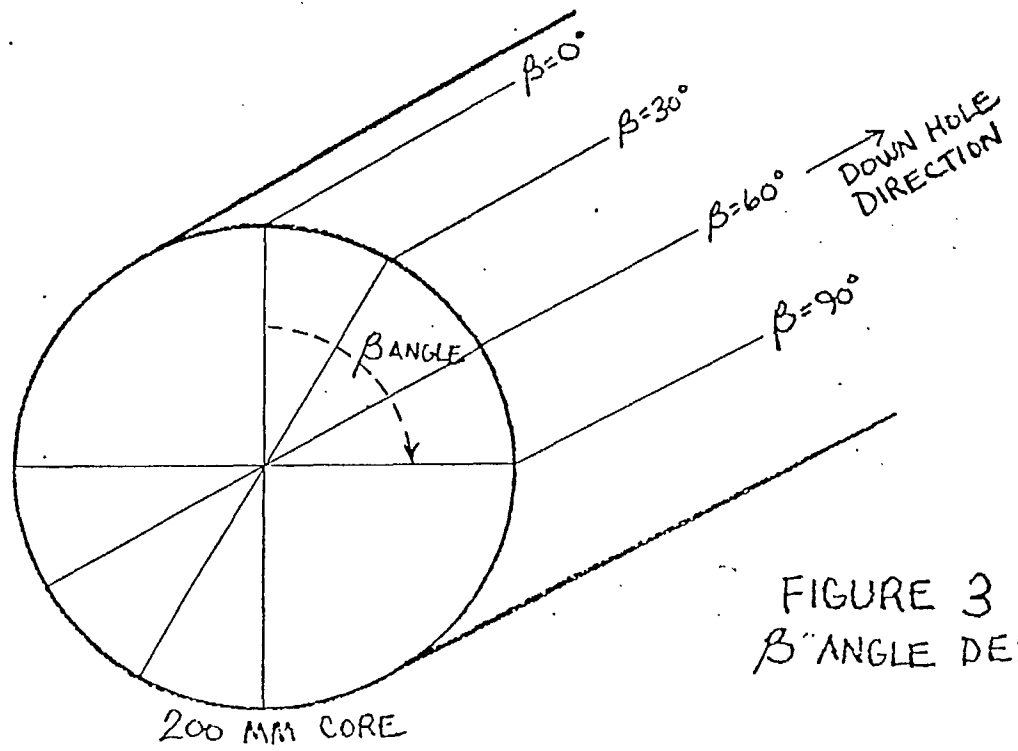


FIGURE 3  
 $\beta$  ANGLE DESIGNATION

TABLE 1  
DRILL HOLE NUMBER 101-S09-MOD1  
3.489 TO 4.422 m

DEPTH (m)	$\alpha$ (From Axial)	$\beta$ (Around Circumference)	DATE DRILLED
3.489	0°	AXIAL	86-06-20
4.190	90°	0°	86-06-20
4.240	90°	30°	86-06-20
4.290	90°	60°	86-06-20
4.340	90°	90°	86-06-20
3.580	30°	0°	86-06-20 *
3.719	30°	90°	86-06-20 *
3.955	60°	0°	86-06-20
4.054	60°	90°	86-06-20 *

\* DESIGNATES DAMAGED CORE

TABLE 2

DRILL HOLE NUMBER 101-S02-M01  
0.749 TO 1.670 m, 1.670 TO 2.275 m

DEPTH (m)	$\alpha$ (From Axial)	$\beta$ (Around Circumference)	DATE DRILLED
0.746	0°	AXIAL	87-07-06
1.320	90°	0°	87-07-06
1.250	90°	30°	87-07-06
1.170	90°	60°	87-07-07
1.105	90°	90°	87-07-07 *
1.045	90°	90°	87-07-07 *

\* DESIGNATES DAMAGED CORE

